IMPROVED DESIGN AND EXPERIMENT OF ANTI-CLAY ADHESION FOR NO-TILLAGE MAIZE PLANTER SEEDING MONOMER
/
玉米免耕机播种单体防黏土改进设计与试验

Min FU*[,1)], Rongfeng LI[1)], Yilin HAO[1)], Fanhua MENG[2)], Jiacheng ZHOU[1)], Chengmeng WANG[1)]
[1)] Northeast Forestry University, College of Mechanical and Electrical Engineering, Harbin / China;
[2)] Heilongjiang DEWO Technology Development Co., Ltd, Harbin / China
Tel: +86 15663688203; E-mail: fumin1996@163.com
DOI: https://doi.org/10.35633/inmateh-70-33

Keywords: *no-tillage seeding; seeding monomer; soil-contacting part; clay soil; TRIZ (Theory of Inventive Problem Solving)*

ABSTRACT
When the seeding monomer of no-tillage maize planter operates in sticky and wet soil, soil bonding and blocking of soil-touching parts will occur to different degrees, leading to functional failure and affecting the quality of seeding operation. Aiming to improve the anti-adhesion property with minimum cost, a seeding monomer is modified to operate in sticky and wet soil with the support of TRIZ (Theory of Inventive Problem Solving). There are two major scheme adjustments, including self-cleaning seedbed collating device and split gauge wheel. The Su-field model of seedbed collating device is constructed, and the design scheme of smaller wavy coulter and dirt scraper is proposed on the basis of the standard-solution tool and water-film theory. And the parameters of the wave are determined on account of force analysis of soil particles and bionic earthworm. Based on the systemic-functional analysis of the seeding depth-limiting device and the force analysis of gauge wheel during operation, a split type of depth-gauge wheel with large lug hole is designed. As a result, the field trial demonstrates that the improved monomer could meet the operation requirements of clay soil with the water content of 15%-25%. Compared with the original model, the residual clay content is decreased (seedbed collating device 57.5%, gauge wheel seeding depth-limiting device 10%). This study can provide reference for the anti-adhesion design of soil-contacting parts of agricultural machinery.

摘要
玉米免耕播种机的播种单体在黏湿土壤中作业时，各触土部件会发生不同程度的土壤粘结与堵塞，导致功能失效，影响播种作业质量。以最小代价提高抗粘性能为目标，应用 TRIZ 理论辅助分析求解改进方案，设计了一种适于黏湿土壤作业的具有自清洁式种床整理装置、分体式播种限深轮的播种单体。构建了种床整理装置的问题“物-场模型”，基于“标准解工具”和水膜理论提出小波纹形破茬刀盘组合刮土刀的设计方案；通过波纹圆盘破茬刀运动时土壤质点受力分析，结合仿生蚯蚓确定波纹形状参数。基于播种限深装置的“系统功能分析”和限深轮作业过程受力分析，设计了分体式大腰孔限深轮。田间试验表明，改进后的播种单体能够满足含水量在 15%~25%黏壤土的播种作业要求，与原机型相比，种床整理装置和限深装置的残留粘土量分别下降 57.5%、10%。该研究可为农机触土部件抗土壤粘附设计提供参考。

INTRODUCTION
No-tillage Maize Planter is a key tool for the conservation tillage of maize, the composition mainly includes seedbed collating device, seeding depth-limiting device, soil-covering device, etc *(Yalcin et al., 2005; Jia et al., 2017)*. And the operation quality of each soil-contacting device of seeding monomer directly affects the maize yield. During the spring ploughing period in Heilongjiang Province, China, the soil is sticky and wet, hence the soil-contacting parts of the seeding monomer may have different degrees of soil bonding and blocking, which leads to the decline of operation quality.

In recent years, many companies and scholars have conducted in-depth research on seeding monomers. The 1950 series no-tillage maize planter, produced by John Deere in the United States, has seeding monomer with side-position depth-gauge wheel, which can ensure the consistent seeding depth *(Morrison et al., 2002).* The YP series no-tillage maize planter produced by Great Plains has the seeding monomer with wavy coulter and the double-disc furrow opener with non-isometric dislocation arrangement, making the effects of soil-breaking and stubble-breaking better *(Triplett et al., 2008)*.

[1] *Min Fu, Prof.; Rongfeng Li, M.S.Stud.Eng; Yilin Hao, M.S.Stud.Eng; Fanhua Meng, Engineer; Jiacheng Zhou, M.S.Stud.Eng; Chengmeng Wang M.S.Stud.Eng;*

The ED series no-tillage maize planter produced by Amazone in Germany has the seeding monomer adopting the stubble-cutting mode of gravity double-disc furrow opener, and the scalpriform furrow opener installed directly behind the disc can determine the seeding position and the embedment direction of seeds *(Fuentes-Llanillo et al., 2021).* Meanwhile, scholars have also conducted detailed research on the problem of preventing soil adhesion in the soil-touching parts of no-tillers. Jafar Massah, Iran et al. designed corrugated blades by simulating the body geometry of armadillo (*Massah et al., 2020)*. Massah Jafar et al. optimized the design of soil tilling components based on the bionic electro osmosis technology and the biometric features of animal body surface to reduce the adhesion of soil (*Massah et al., 2021)*.

In the 1990s, the no-tillage maize planter was introduced in China, and local improvements were made according to actual demands. Zhao et al. designed a profiling compacting device of seeding monomer that is suitable for hilly areas and established an interaction model between compacting device and soil, which combined with the characteristics of the soil *(Zhao et al., 2017)*. Gao et al. proposed a method of down-force control of seeding monomer based on the pressure of airbag and the dip angle of profiling four-bar linkage, which was used to precisely control the seeding depth *(Gao et al., 2019)*. Jia et al. designed an anti-blocking stubble-breaking machine for inter-row no-tillage, using the intermittent arrangement of cutter teeth with high cutting effect and low soil adhesion *(Jia et al., 2013)*. Hou et al. designed the seeding monomer of double-DOF multi-articulated profiling no-tillage machine, with ploughshare-type furrow opener and separate soil-covering device as well as compacting device *(Hou et al., 2019).* The soil-covering and compacting wheel of seeding monomer designed by Guo et al. adopted the conical wheel structure, which can realize soil-covering and compacting at one time *(Guo et al., 2017).*

The above research provides useful references for the improved design of no-tillage maize planter seeding monomer, however, the research on the causes of failure of soil-contacting parts in sticky and wet soil as well as the anti-adhesion design of seeding monomer are still not sufficient. In this paper, TRIZ (Theory of Inventive Problem Solving) is used to analyse the failure causes, identify critical imperfections and improving directions *(Altshuller, 1984).* Combined with the force analysis of the seeding process, the seeding monomer with self-cleaning seedbed collating device and split gauge wheel is designed. The implementation effect of the improved scheme is verified by field trials.

MATERIALS AND METHODS

Overall Structure

The seeding monomer structure of commonly used traction-type no-tillage maize planter is shown in Fig. 1, which is mainly composed of wavy coulter, four-bar linkage, double-disc furrow opener, depth-gauge wheel, support arm, soil-covering wheel, etc.

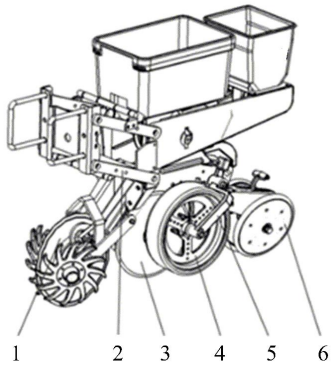

Fig. 1 - Schematic diagram of the seeding monomer of no-tillage maize planter

1. wavy coulter; 2. four-bar linkage; 3. double-disc furrow opener; 4. gauge wheel; 5. support arm; 6. soil-covering wheel

Operating Principle

The seeding monomer of no-tillage maize planter is hooked up to the whole machine frame and is towed by the tractor for work *(Lin et al., 2015).* During the seeding operation, the wavy coulter cuts into the soil, as well as cuts the stubble and straw on the seeding path to complete the collation of seedbed. Then, the double-disc furrow opener cuts the soil along the seeding path to form a seeding furrow, and the seed-metering device sends maize seeds to the bottom of the seeding furrow to complete the seeding operation. The soil-covering wheels arranged in a V-shape squeezes the soil on both sides of the seeding path into the seeding furrow. The soil-covering wheel rolls and compacts to complete the operation.

Problems in the Operation of Sticky and Wet Soil

The seeding monomer can successively realize the functions of seedbed collating, depth-limiting furrow seeding, and soil-covering compacting, etc. The soil-contacting parts include wavy coulter, gauge wheel, double-disc furrow opener and soil-covering wheel *(Wang et al., 2021; Fu et al., 2022).* When working in the sticky and wet soil, each soil-contacting part is in direct contact with the soil, resulting in different degrees of soil adhesion problems (see Fig. 2).

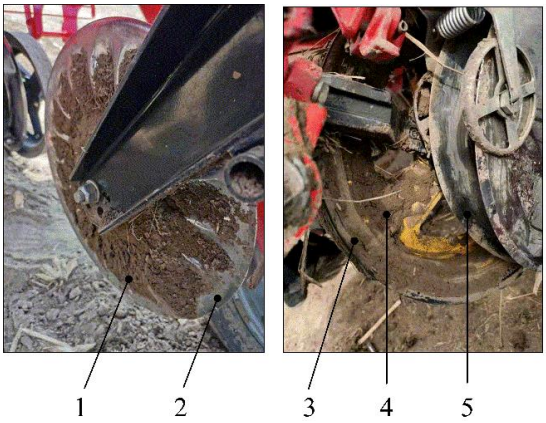

*(**a**) Actual bonding situation of corrugated cutter head* *(**b**) Actual bonding situation of gauge wheel*

Fig. 2 - Actual bonding situation in soil-contacting parts of seeding monomer.

1. clay on wavy coulter; 2. wavy coulter; 3. gauge wheel; 4. clay on gauge wheel; 5. double-disc furrow opener

Improved Design of Seeding Monomer Based on TRIZ

TRIZ is a systematic and structured innovation methodology *(Altshuller, 1984)*. It is effective in breaking through inertial thinking, inspiring innovative consciousness, expanding design ideas, assisting innovation designs, and solving technical problems *(Kang et al., 2022; Fu, 2021)*. In this paper, TRIZ is applied to analyse the soil-adhesion problem of the soil-contacting part of seeding monomer, with the goals of improving the anti-adhesion property at the minimum cost and solving the scheme of improved design.

Improved Design of Wavy Coulter Based on Su-Field Analysis

Coulter is the core component of seedbed collating device, and its function is to cut stubble and straw on the seeding path, so as to provide a favourable seedbed for the germination and growth of seeds *(Gao, 2002; Gao et al., 2008; Liao et al., 2004).* When operating in clay soil, the wavy coulter bond to the soil and accumulate continually, leading to the increase of soil movement and power consumption. The Su-field model of the problem, as shown in Fig. 3, shows that the clay soil has a harmful adhesion effect on the wavy coulter.

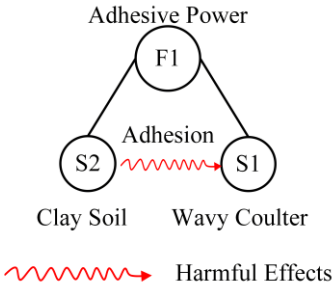

Fig. 3 - Analysis of Su-Field model of the wavy coulter

The standard solution S1.2.2 in TRIZ, that is, the introduction of the deformation of S1 or S2, is applied to eliminate the harmful effects *(Fu, 2021)*, and the improved conceptual scheme 1, that is, the change of configuration and parameter of the wavy coulter (i.e. deformation of S1) is proposed. According to the water-film theory, the adhesion of soil to metal is related to the contact area of soil and metal parts, the larger the contact area, the easier it is to form a water-film layer and the greater the adhesion of clay soil *(Zuo et al., 1997; Zheng, 2019)*. The smaller wavy coulter can reduce the contact area with the clay soil and avoid the formation of a continuous water film interface, thus reducing the adhesion amount of soil.

The standard solution S1.2.1 in TRIZ, that is, the introduction of S3, is applied to eliminate the harmful effects *(Fu, 2021)*, and the improved conceptual scheme 2, that is, adding a scraper, is proposed to scrape away the attached clay soil on the disc surface.

Design on Structure and Key Parameters of the Improved Scheme

1) Overall Structure and Anti-adhesion Operating Principle

The structure of the seedbed collating device with anti-adhesion property designed by the improved conceptual solution is shown in Fig. 4. The rack and weeding machine of improved seedbed collating device adopt original structure, and change the configuration and parameter of the wavy coulter so as to reduce the contact area with soil. Besides, cambered scraper is added to the racks on both sides of wavy coulter, aiming to scrape away the clay attached on the disc surface.

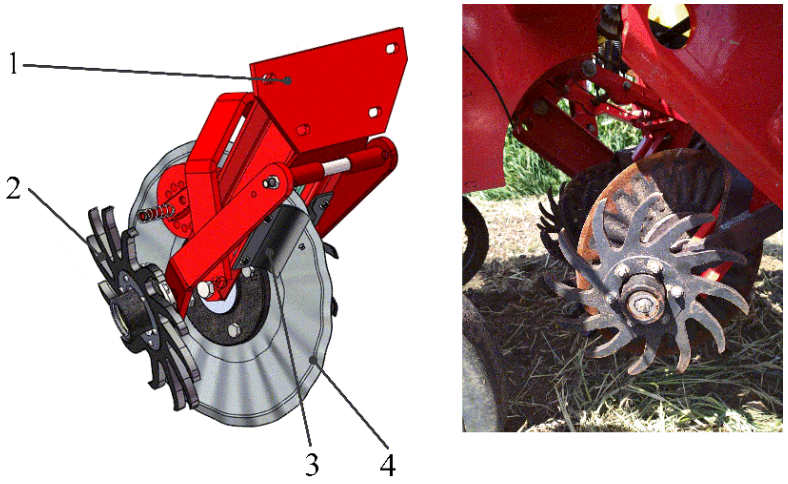

(a) 3D model *(b) Physical model*

Fig. 4 - Structure of improved wavy coulter

1. racks; 2. assembly of weeding wheel; 3. cambered scraper; 4. modified-wavy coulter

2) Design of Key Parameters of Improved Scheme

According to the agronomic requirements of stubble cutting and rod cutting, the modified-wavy coulter is determined as 400 mm in diameter, 4 mm in thickness and 65 Mn in material. The corrugation on the surface of coulter is formed by stamping. In this paper, the corrugation parameters are determined by the force analysis of soil particles *(Wan et al., 2014; Bai et al., 2014)* (see Fig. 5) during the movement of soil and the wavy coulter.

The resultant force at the force point Q is mainly generated by the friction between clay soil and the wavy coulter as well as the mutual extrusion of the two. From Fig. 5, the three component forces of the resultant force F_n are:

$$F_c = F_n \cos\alpha \cos\beta \quad (1)$$

$$F_a = F_c \tan\beta \quad (2)$$

$$F_z = \frac{F_c \tan\alpha}{\cos\beta} \quad (3)$$

When the no-tillage machine is operating at a constant speed, the angular velocity at point Q is invariable, hence the torque at point Q is unchanged. As a result, the circumferential force F_c at point Q is constant. To reduce the amount of soil adhesion, the lateral force F_z and radial force F_a should be reduced.

It can be seen from Equation (2) that the smaller the angle β, the smaller the radial force F_a. If the angle $\beta = 0°$ then the radial force $F_a = 0$, which can eliminate the adhesive attraction of soil to the wavy coulter along the radial direction.

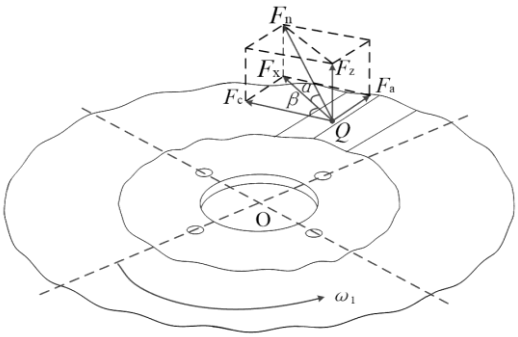

Fig. 5 - Force analysis of soil particles during the movement of wavy coulter

1. raised corrugation; 2. wavy coulter; Q is the force point, O is the centre of rotation.

F_c is circumferential force; F_a is radial force; F_z is lateral force; F_n is the resultant force at the point Q; F_x is the horizontal component of the force F_n; α is the angle between the force F_n and the force F_x. β is the angle between force F_c and force F_v.

The configuration of wave crest directly affects the anti-adhesion property and operation resistance *(Zeng et al., 2018)*. At present, the commonly used corrugated configuration is cambered wave crest. Since the area of arc between two points (lines) is larger than the area of plane, it is easier to form water-film to produce the adhesion phenomenon. In this paper, the plane shape of wave crest is used for structural design. When the angle β = 0 °, the stress state of the two crest surfaces is shown in Fig. 6.

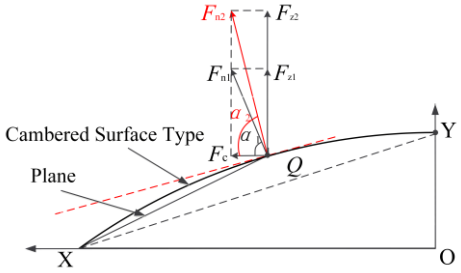

Fig. 6 - Stress states of two wave crests surfaces

Q is the force point, O is the centre of symmetry. F_c is the circumferential force; F_{n1} is the resultant force at point Q of the plane wave crest; F_{n2} is the resultant force at the point Q of the cambered wave crest; F_{c1} is the lateral force at the point Q for plane wave crests; F_{c2} is the lateral force at the point Q for cambered wave crests; α_1 is the angle between the force F_{n1} and the force F_c. α_2 is the angle between the force F_{n1} and the force F_c.

From Equation (3), it can be seen that the smaller the angle α, the smaller the lateral force F_z on the Q point. It can be seen from Fig. 6 that since the angle α_1 is smaller than the angle α_2, the lateral force F_{z1} on the plane wave crest is smaller than the lateral force F_{z2} on the cambered wave crest, which can reduce the soil adhesion to the wavy coulter along the normal direction.

The structure of the plane wave crest is determined by the wave height h and the wave width b. The local structure and stress state of the plane wave crest are shown in Fig. 7.

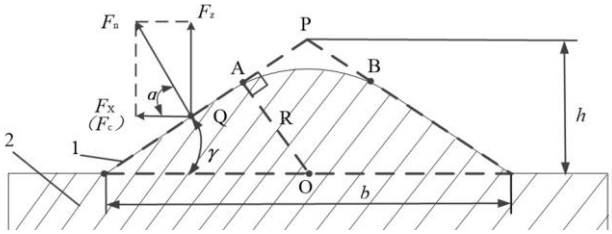

Fig. 7 - Local structure and stress state of the plane wave crest

1. surface of wave crest; 2. coulter

Q is the force particle; h is the wave height; b is the wave width; F_n is the resultant force at the point Q; F_x is the horizontal component of the force F_n; F_c is the circumferential force; α is the angle between the force F_n and the force F_x. γ is the angle between the crestal plane of corrugation and the horizontal plane. O is the arc centre of wave crest. R is the arc radius of wave crest.

From Fig. 7, it can be seen that the angle between the crestal plane of corrugation and the horizontal plane γ is:

$$\gamma = \arctan\frac{2h}{b} \tag{4}$$

Earthworm, as a soil organism, has excellent anti-adhesion property. This paper uses bionic earthworm to determine the corrugation configuration parameters.

According to the characteristics of earthworm skin shape, the ratio of wave height h to wave width b is 1:3 *(Ma et al., 2014)*. Take h=9 mm *(Wei et al., 2017)*, b=27 mm, and substitute them into Equation (4) to get $\gamma \approx 34^{o}$.

Considering the requirements of stamping process and reducing operation resistance, the wave crest needs to be chamfered, and the radius of chamfering arc R is:

$$R = \frac{b}{2}\sin\gamma \tag{5}$$

Substituting b=27 mm, $\gamma \approx 34^{o}$ into Equation (5) yields R=7.55 mm.

The structural parameters of the modified-wavy coulter are compared with the original coulter, as shown in Table 1. The comparison of the physical drawing is shown in Fig. 8.

Table 1

Parameters of wavy coulter

Structural style	Cutter diameter (mm)	Wave height (mm)	Wave width (mm)	Corrugated surface Form
Original-wavy coulter	400	15	30	Cambered type
Modified-wavy coulter	400	9	27	Plane type

(a) original-wavy coulter *(b) modified-wavy coulter*

Fig. 8 - The Physical drawing comparison

Improved Design of Seeding Depth-limiting Device Based on Systemic-Functional Analysis

The function of the seeding depth-limiting device is to carry the operating weight of the seeding monomer and to control the depth of the furrow opener cutting into the soil. In this paper, the systemic-functional analysis in TRIZ is used to analyse the functional structure of the depth-limiting device, identify critical defects, and search for improved scheme on solving the problem of soil adhesion.

Name of system: seeding depth-limiting device.

Function of system: control the depth of seeding.

Object of system: soil.

Components of system: seeding monomer racks, double-disc furrow opener, integrated gauge wheel, support arm, depth-adjusting handle, scraper on seeding furrow opener, scraper on gauge wheel circumference.

Components of super-system: whole machine racks, sticky soil.

The functional relationships among functional objects, system components and super-system components are analysed, and the systemic-functional model diagram of seeding depth-limiting device is established (see Fig. 9).

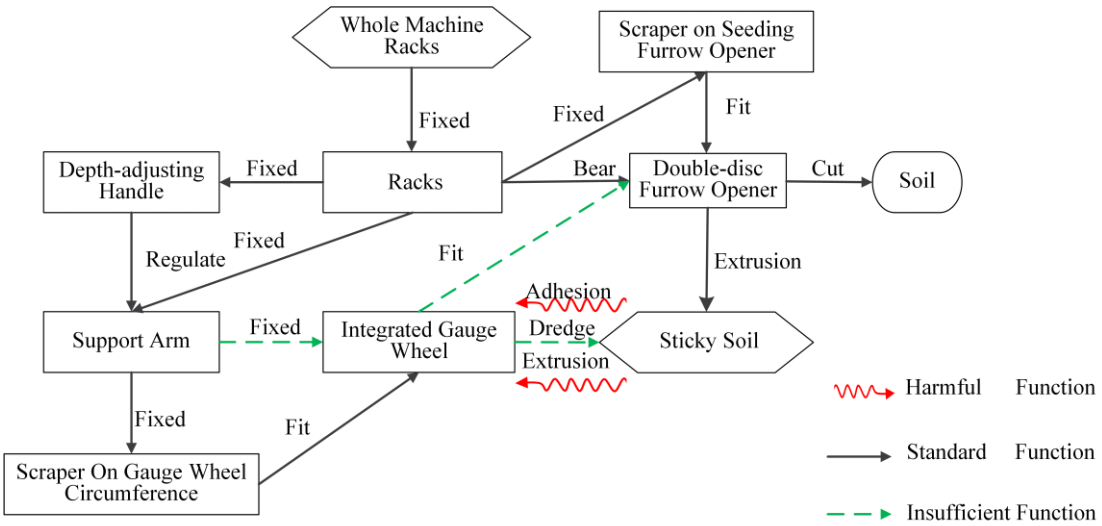

Fig. 9 - Systemic-functional analysis of depth-limiting device

From Fig. 9, it can be seen that the seeding depth-limiting device has five critical defects. The integrated gauge wheel is a key component to solve the anti-adhesion problem of seeding depth-limiting device. Therefore, conceptual scheme 3 is proposed to improve the structure of the integrated gauge wheel and its manner of supporting and fixing.

Improved Design of the Structure of Gauge Wheel

(1) Integrated Gauge Wheel Structure of the Original Model

The structure of the integrated gauge wheel of the original model is shown in Fig. 10. The hub and spokes are formed all-in-one by stamping steel plate, and the wheel body is covered with three lug holes.

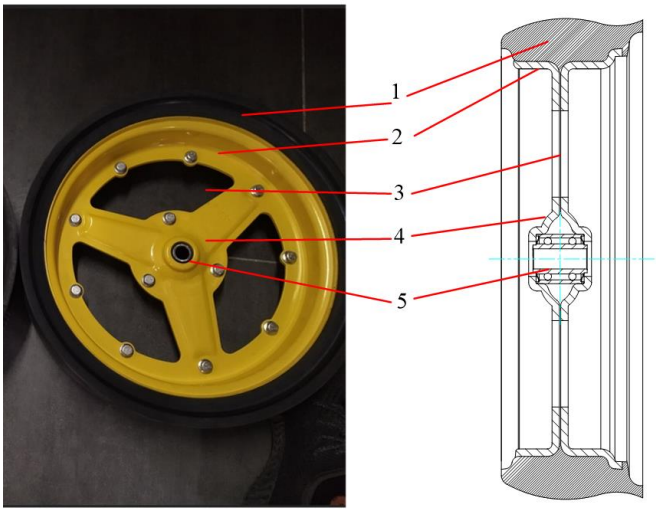

(a) Physical model *(b) Cutaway view*

Fig. 10 - Structure of integrated gauge wheel

1. tire; 2. wheel hub; 3. lug hole; 4. wheel spokes; 5. bearing

(2) Force Analysis of Integrated Gauge Wheel during Operation

When operating on sticky and wet soil, the position of clay soil of the integrated gauge wheel is located between the furrow opener and gauge wheel, and the maximum extrusion force of clay soil on the hub of the gauge wheel is formed at the maximum soil-separation position of the furrow opener (see Fig. 11a.).

In order to balance the maximum extrusion force, a pair of equilibrium moments around point O are generated at the connection points A and C of the gauge wheel. After decomposition and transmission, radial extrusion force is formed on points A and C, and axial extrusion force is formed on points B and D. The force analysis is shown in Fig. 11 (b).

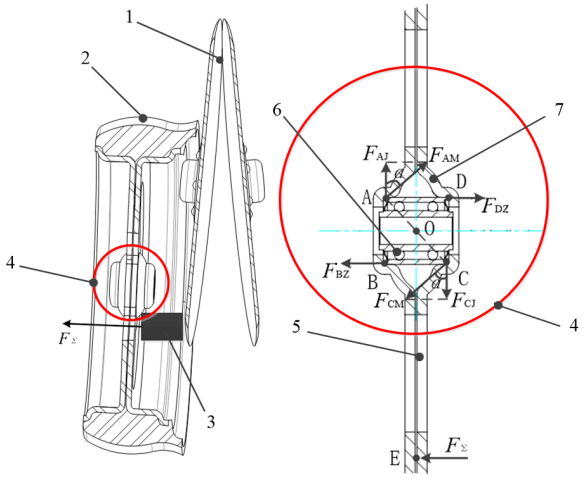

(a) Position of soil extrusion force *(b) Force analysis of connection position*

Fig. 11 - Soil-adhesion position and force analysis of integrated gauge wheel

1. double-disc furrow opener; 2. integrated gauge wheel; 3. clay soil; 4. connecting parts; 5. lug hole; 6. Bearing; 7. integrated hub

A, B, C, D are the four force points. O is the centre of deflection torque. E is the action point of extrusion force. F_{Σ} is the soil extrusion force. F_{AJ} is the radial force at A. F_{AM} is the deflecting force at A. F_{BZ} is the axial force at B. F_{BJ} is the radial pressure at B. F_{CM} is the deflecting force at C. F_{CJ} is the radial-deflecting component force at C. F_{DZ} is the axial force at D.

Assuming that the fixed axis of the gauge wheel is absolutely rigid. Set the distance between OE as L_1, $OC = OA$ as L_2, the following relationship can be obtained from Fig. 11(b).

$$F_{\Sigma} L_1 = F_{AM} L_2 = F_{CM} L_2 \tag{6}$$

According to Fig. 11(b) and Equation (6), the forces acting on each local contact position can be obtained as follows.

Radial force at point A:

$$F_{AJ} = \frac{F_{\Sigma} L_1}{L_2} \cos\alpha \tag{7}$$

Axial force at point B:

$$F_{BZ} = \frac{F_{\Sigma} L_1}{L_2} \sin\alpha \tag{8}$$

Radial force at point C:

$$F_{CJ} = \frac{F_{\Sigma} L_1}{L_2} \cos\alpha \tag{9}$$

Point D axial force:

$$F_{DZ} = \frac{F_{\Sigma} L_1}{L_2} \sin\alpha \tag{10}$$

As can be seen from Fig. 11 (a), the extrusion force of sticky soil is generated by the small area of lug hole on the gauge wheel and the weak dredging ability of sticky soil, which in turn forms the deflection torque. As shown in Fig. 11 (b), since the bearing hole of the integrated gauge wheel spoke is in local contact with both ends of the bearing, deformation occurs at the fit of the two ends under the extrusion force of constantly changing size and direction, resulting in a larger aperture at the fitting location, as well as making the gauge wheel detach from the fixed support arm.

From Equation (7) to Equation (10), it can be seen that the harmful extrusion forces on the integrated gauge wheel and the fitting location of bearings are all formed by the conversion of the extrusion force F_{Σ} of sticky soil.

Through the above analysis, it can be clear that the following weaknesses are supported to be improved: ① the fitting forms of the depth-limiting spoke and bearings need to be improved to enhance the connection strength. ② the form of the lug hole of the gauge wheel needs to be improved to enhance the dredging ability of sticky soil, hence reduce or eliminate the extrusion force F_{Σ}.

(3) Structure of Split Gauge Wheel

The structure of the improved split gauge wheel is shown in Fig. 12. In view of the two weaknesses mentioned in the previous section, the gauge wheel spoke and hub adopt split structure. The hub and spoke are joint by bolt groups to maximize the area of the lug hole. According to Newton's Third Law, as the area of the lug hole increases, the obstruction to clay soil decreases. Therefore, no clay soil can be formed between the gauge wheel and the double-disc furrow opener, and no extrusion force on the gauge wheel can be generated, thus the stability of the depth-limiting device in the operation of sticky and wet soil can be improved.

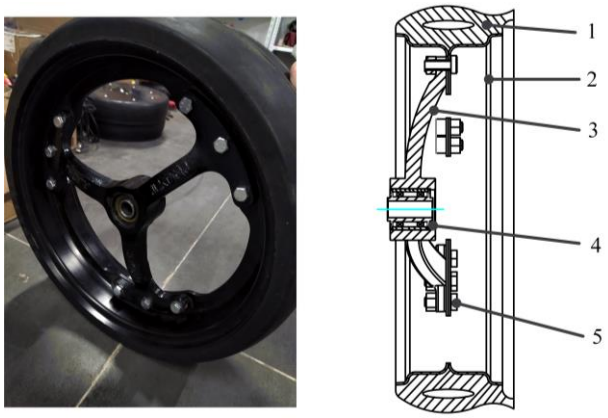

(a) Physical drawing *(b) Cutaway view*

Fig. 12 - Structure of split gauge wheel

1. tires; 2. hubs; 3. spokes; 4. bearings; 5. bolts

Improved Design of the Overall Structure of Seeding Monomer

The improved 3D model of the seeding monomer is shown in Fig. 13(a), and the physical prototype is shown in Fig. 13(b). The weight of the seeding monomer is 160 kg, and the boundary dimensions are 1580 mm × 1127 mm × 343 mm.

(a) 3D model *(b) Physical model*

Fig. 13 - Improved seeding monomer

For the improved seeding monomer, the configuration and parameters of the wavy coulter is changed, and a cambered scraper to remove the sticky soil on the disc surface is added. The integrated gauge wheel of the depth-limiting device is improved into a split gauge wheel, that is, the spoke and hub of the gauge wheel adopt a split structure, while the contact area between the mating hole of spoke bearing and the outer-ring of bearing is increased to improve the strength of the connection support. The area of the lug hole is increased to reduce the obstruction of sticky soil, and the independent regulation of left and right gauge wheels is changed into an integrated linkage mode.

Conditions for Trials

In April 2022, the verification trial was conducted in the experimental field of Devo Group, Shuangcheng District, Harbin City, Heilongjiang Province (126°52′, 45°53′), China. The original and improved seeding monomers were hooked up to the 2BMQ-2 no-tillage maize planter at the same time, and field trials were conducted in designated areas of the experimental field.

Method for Trials

Due to the different functions of each soil-contacting part, different experimental methods should be adopted. A comparative trial is carried out on the seedbed collating device. The two improved schemes of modified-wavy coulter as well as modified-wavy coulter and dirt scraper are compared with the original model, and the clay weight of the wavy coulter for three schemes are recorded.

A mixed orthogonal test with three factors and three levels is used for the seeding depth-limiting device, with 17 sets of tests for each device. Each group of tests is operated continuously for one hour. After collecting the residual clay soil inside the gauge wheel hub, the weight statistics are made. The improved performance of seeding depth-limiting device is evaluated according to the weight of the residual clay soil.

The seeding depth-limiting device takes the clay amount y_1 inside the wheel hub as the test index. The relative water content of soil A, the operating speed B, and the lug hole area of gauge wheel C are selected as the test factors. According to agronomic requirements, the range of relative water content of soil is from 15% to 25%, so the level of test factor A is proposed to be 15%, 20%, and 25%. The speed range of field operation of 2BMQ-2 no-tillage maize planter is from 6 km/h to 8 km/h, so the level of test factor B is proposed to be 6 km/h, 7 km/h, 8 km/h. The current gauge wheel is mainly no-lug hole or integrated semi-open lug hole structure. The improved split open-lug hole is designed in this paper, whose area is 5×10^4 mm^2, so the level of test factor C is proposed to be 0 mm^2 (no-lug hole), 2.7×10^4 mm^2 (lug hole area of the original model), 5×10^4 mm^2. The level coding of test factors is shown in Table 2.

Table 2

Coding table of factor levels

Level	1	2	3
Water content A/ (%)	15	20	25
Operating speed B/(km/h)	6	7	8
Lug hole area C/ (mm^2)	0	2.7×10^4	5×10^4

Test method of test index: Take the amount of soil-adhesion as the test index. After each test, use a soil-spade to clear and collect the clay soil at the inner side of the gauge wheel hub, then use spring scales to weigh separately. Each group of tests should be repeated three times to get the mean value.

RESULTS

Trial Results

The results of comparative trials of seedbed collating device are shown in Table 3. The results show that the amount of soil-adhesion adopted by scheme of modified-wavy coulter and dirt scraper is reduced by 57.5%, compared with that of original model.

Table 3

The clay amount of seedbed collating device

Time/h	0.5	1	1.5
Modified-wavy coulter combination scraper/ (g)	708	787	852
Modified-wavy coulter /(g)	721	973	1250
Original- wavy coulter / (g)	924	1632	1978

The results of comparative trials of gauge wheel of the depth-limiting device is shown in Fig. 14.

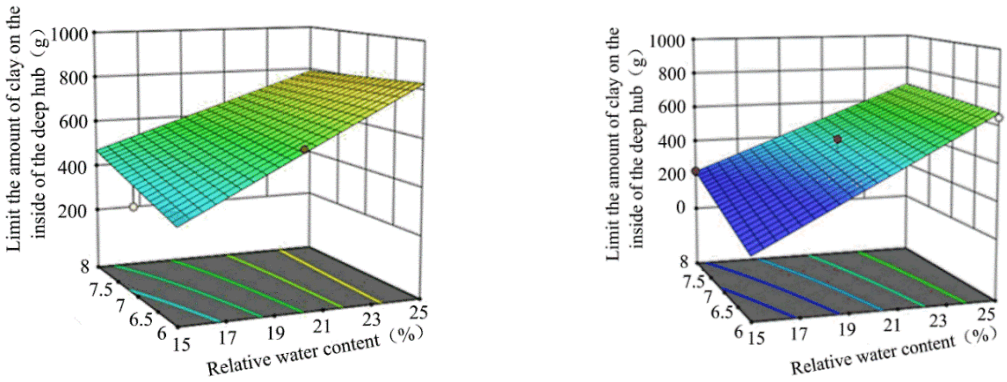

(a) Lug hole area is 5×10^4mm^2 *(b) Lug hole area is 2.7×10^4mm^2*

Fig. 14 - Response surface diagram of clay with different lug hole areas

The results show that when the lug hole area of the gauge wheel is 5×10^4 mm^2, the amount of soil-adhesion decreases by about 10%, compared with 2.7×10^4 mm^2 of the original model.

CONCLUSIONS

Regarding soil-adhesion problem of no-tillage maize planter in black soil area of China, a reformed design of seeding monomer of no-tillage maize planter was constructed with minimum cost and support of TRIZ analysis. In contrast with original version planter, the level of soil adhesion decreased 57.5% in seedbed collating device and 10% in seeding depth-limiting device. This result fulfils the prerequisite for seeding in sticky and wet soil.

The main contributions of the current research can be concluded as follows.

(1) Aiming at the problem that the soil-adhesion of wavy coulter leads to an increase in the disturbance of soil and a loss of crushing function on the surface soil, a self-cleaning seedbed collating device is designed based on Su-field analysis of TRIZ. In the design, a small wavy coulter is used, and a scraper is added on the surface of blades. The parameters of wavy coulter are determined by combining bionic earthworms and the force analysis of soil particle in motion. The results of field trials demonstrate that the modified coulter with scraper has the least amount of clay soil.

(2) Focusing on the problem that the depth-gauge wheel loses its function due to the accumulation and extrusion of clay, the spoke and hub are designed in a split type based on the systemic-functional analysis of TRIZ and the force analysis of the depth-gauge wheel operation process. The depth-gauge wheel of the structure increases the area of lug hole to reduce the adhesion and compression of the soil and changes the independent regulation of the left and right gauge wheels into an integrated linkage mode. The results of field trials show that the most significant factors affecting the soil-adhesion of gauge wheel are the water content of soil as well as the area of lug hole, and the improved split large-lug hole gauge wheel has the least amount of soil-adhesion.

Field trials demonstrate that, the designed self-cleaning seedbed collating device and large-lug hole gauge wheel, can effectively improve the operation performance of no-tillage maize planter, which has market promotion value in the black soil area of northeast China, and also has been recognized by the vast number of customers in China (Qingdao) Agricultural Machinery EXPO. However, China has a vast territory with large land differences and low degree of large-scale agricultural mechanization. The future research and development of no-tillage maize machines and tools are supposed to be closely related to soil conditions in various regions, which will certainly bring great challenges to the product versatility of agricultural equipment enterprises. The author will further study the generalization, modularization and adaptation of equipment based on the agronomic differences of soil and maize seeding in different regions.

ACKNOWLEDGEMENT

This paper was funded by the National Natural Science Foundation of China [Grant No. 51975114] and the Natural Science Foundation of Heilongjiang province of China [Grant No. LH2019E003].

REFERENCES

[1] Altshuller, G.S. (1984). *Creativity as an exact science: the theory of the solution of inventive problems*. Gordon and Breach Science Publishers: New York, USA, pp.15-20.

[2] Bai, X.H., Lin, J., Lv, C.Y., & Hu, Y.Q. (2014). Analysis and experiment on working performance of disc coulter for no-tillage seeder (免耕播种机圆盘破茬刀工作性能分析与试验). *Transactions of the Chinese Society of Agricultural Engineering*, China, 30(15), 1-9.

[3] Fu M. (2021). *Systematic Innovation Approach - TRIZ Practical Tutorial* (系统化创新方法-TRIZ 实用教程); Northeast Forestry University Press: Harbin, China, pp.5-10.

[4] Fu, M., Hao, Y.L., Gao, Z.F., Chen, X.Q., & Liu, X.Y. (2022). User-Driven: A Product Innovation Design Method for a Digital Twin Combined with Flow Function Analysis. *Processes*, Switzerland, 10(11), 2353.

[5] Fuentes-Llanillo, R., Telles, T. S., Junior, D. S., de Melo, T. R., Friedrich, T., & Kassam, A. (2021). Expansion of no-tillage practice in conservation agriculture in Brazil. *Soil and Tillage Research*, Netherlands, 208, 104877.

[6] Gao, Y.Y., Wang, X., Yang S., Zhao, X.G., Dou, H.J., & Zhao, C.J. (2019). Design and test of pneumatic downforce control system for planting (播种机气动式下压力控制系统设计与试验). *Transactions of the Chinese Society for Agricultural Machinery*, China, 50(07), 19-29+83.

[7] Gao, H. (2022). *Agricultural mechanization production science* (农业机械化生产学); China Agricultural Press: Beijing, China, 2002; pp.20-25.

[8] Gao, H.W., Li, H.W., & Yao, Z.L. (2008). Study on the Chinese light no-till seeders (我国轻型免耕播种机研究). *Transactions of the Chinese Society for Agricultural Machinery*, China, 39(04), 78-82.

[9] Guo, H., Chen, Z., Jia, H.L., Zheng, T.Z., Wang, G., & Wang, Q. (2017). Design and experiment of soil-covering and soil-compacting device with cone-shaped structure of wheel (锥形轮体结构的覆土镇压器设计与试验). *Transactions of the Chinese Society of Agricultural Engineering*, China, 33(12), 56-65.

[10] Hou, S.Y., Chen, H.T., Shi, N.Y., Zou, Z., Ji, W.Y., & Wang, Y.C. (2019). Design and experiment of two-degree-of-freedom multi-articulated profiling no-tillage precision design and experiment of two-degree-of-freedom multi-articulated profiling no-tillage precision drill unit (双自由度多铰接仿形免耕精量播种单体设计与试验). *Transactions of the Chinese Society for Agricultural Machinery*, China, 50(04), 92-101.

[11] Lin J., Qian W., Li B.F., & Liu, Y.F. (2015). Simulation and validation of seeding depth mathematical model of 2BG-2 type corn ridge planting no-tillage maize planter (2BG-2 型玉米垄作免耕播种机播种深度数学模型的仿真与验证). *Transactions of the Chinese Society of Agricultural Engineering*, China, 31(09), 19-24.

[12] Jia, H.L., Wang, W.P., Chen, Z., Zheng, T.Z., Zhang, P., & Zhuang, J. (2017). Research status and prospect of soil-engaging components optimization for agricultural machinery (农业机械触土部件优化研究现状与展望). *Transactions of the Chinese Society for Agricultural Machinery*, China, 48(07), 1-13.

[13] Jia H.L., Zhao J.L., Jiang X.M., Jiang, T.J., Wang, Y., & Guo, H. (2013). Design and experiment of anti-blocking mechanism for inter-row no-tillage seeder (行间免耕播种机防堵装置设计与试验). *Transactions of the Chinese Society of Agricultural Engineering*, China, 29(18): 16-25.

[14] Jin, Y.F., Qin, H.T., Zhang, R.H., Wang, M.Y., Liao, H., & Zhu, S. (2014). Design and test of biaxial rotary duplex operation machine for paddy field and dry-land (水旱两用双轴旋耕复式作业机的设计与试验). *Journal of Chinese Agricultural Mechanization*, China, 35(06), 13-16.

[15] Kang, C. Q., Ng, P. K., & Liew, K. W. (2022). A TRIZ-Integrated Conceptual Design Process of a Smart Lawnmower for Uneven Grassland. Agronomy, Switzerland, 12(11): 2728.

[16] Liao, Q.X., Gao, H.W., & Shu, C.X. (2004). Present situations and prospects of anti-blocking technology of no-tillage planter (免耕播种机防堵技术研究现状与发展趋势). *Transactions of the Chinese Society of Agricultural Engineering*, China, 20(01), 108-112.

[17] Ma, Y.H., Ma, S.H., Jia, H.L., Liu, Y.C., Peng, J., & Gao, Z.H. (2014). Measurement and analysis on reducing adhesion and resistance of bionic ripple opener (仿生波纹形开沟器减黏降阻性能测试与分析). *Transactions of the Chinese Society of Agricultural Engineering*, China, 30(05), 36-41.

[18] Massah, J., Fard, M.R., & Aghel, H. (2021). An optimized bionic electro-osmotic soil-engaging implement for soil adhesion reduction. *Journal of Terramechanics*, Switzerland, 95, 1-6.

[19] Massah, J., Roudbeneh, F.H., Roudbeneh, Z.H., & Vakilian, K.A. (2020). Experimental investigation of bionic soil-engaging blades for soil adhesion reduction by simulating Armadillidium vulgare body surface. *INMATEH-Agricultural Engineering*, Romania, 60(1), 99-106.

[20] Morrison, J.E. (2002). Development and future of conservation tillage in America. *Journal of Research and Applications in Agricultural Engineering*, Poland, 47(1), 5-13.

[21] Triplett Jr, G. B., & Dick, W. A. (2008). No-tillage crop production: A revolution in agriculture! *Agronomy journal*, USA, 100, S153-S165.

[22] Wang, Q.J., Cao, X.P., Wang, C., Li, H.W., He, J., & Lu, C.Y. (2021). Research progress of no /minimum tillage corn seeding technology and machine in northeast black land of China (东北黑土地玉米免少耕播种技术与机具研究进展). *Transactions of the Chinese Society for Agricultural Machinery*, China, 52(10), 1-15.

[23] Wei, L.J., Ku, G.H., & Yin, X.P. (2017). Design and optimization of a new wavy coulter (新型波纹式圆盘破茬刀的设计与优化). *Jiangsu Agricultural Sciences*, China, 45(04), 166-168+176.

[24] Yalcin, H., Cakir, E., & Aykas, E. (2005). Tillage parameters and economic analysis of direct seeding, minimum and conventional tillage in wheat. *Journal of Agronomy*, Pakistan, 4(4): 329-332.

[25] Zeng, Z.W., & Chen, Y. (2018). The performance of a fluted coulter for vertical tillage as affected by working speed. *Soil and Tillage Research*, Netherlands, 175: 112-118.

[26] Zhao, S.H., Liu, H.J., Tan, H.W., Yang, Y.Q., & Zhang, X.M. (2017). Design and experiment of bidirectional profiling press device for hilly area (丘陵地区双向仿形镇压装置设计与试验). *Transactions of the Chinese Society for Agricultural Machinery*, China, 48(04), 82-89.

[27] Zheng, K. (2019). Research status and prospect of soil anti-adhesion technology for tillage equipment (耕整机械土壤减粘脱附技术研究现状与展望). *Journal of Anhui Agricultural University*. China, 46(04), 728-736.

[28] Zuo, C.C., Zhang, S.Q., Ma, C.L., & He, H.P. (1997) The study on the adhesion-decreasing and resistance-reducing of disc opener (圆盘开沟器减粘降阻的试验研究). *Transactions of the Chinese Society for Agricultural Machinery*, China, 28(S1), 41-44.